Semenogelins in the human retina: Differences in distribution and content between AMD and normal donor tissues

Vera L. Bonilha[a,*], **Mary E. Rayborn**[a], **Karen G. Shadrach**[a], **Yong Li**[a], **Åke Lundwall**[b], **Johan Malm**[b], and **Joe G. Hollyfield**[a]

a*Department of Ophthalmology, The Cole Eye Institute, Cleveland Clinic Lerner College of Medicine , Cleveland, OH, 44195, USA*

b*Department of Laboratory Medicine, Lund University, University Hospital, MAS, S-205 02 Malmö, Sweden*

Abstract

The two cellular targets of interest in age-related macular degeneration (AMD) are the photoreceptors and the RPE. However, the mechanisms involved in AMD pathology are not yet fully understood. In the present report, we extend our previous studies on semenogelin proteins (Sgs) in normal human retina and compare these with the distribution in retinas from AMD donor eyes. Semenogelin I (SgI) and II (SgII) are the major structural protein components of semen coagulum, but have been recently found in non-genital tissues as well. Cryo and paraffin sections of human retina were processed for both immunofluorescence and DAB reaction with a specific antibody. The presence of SgI was analyzed in retina and RPE total lysates and SgI was detected by western blot in human retina and RPE. The intensity of immunoreactivity was significantly reduced in the AMD eyes. SgI is expressed in the normal human retina and in the retina of AMD donor eyes, where localization was detected in the photoreceptors and in a few ganglion cells. We find the distribution of SgI in the AMD retinas substantially lower than observed in normal retina. SgI localization to photoreceptors and the RPE suggests a possible function related to the ability of these cells to sequester zinc.

Keywords

Semenogelins; zinc; immunohistochemistry; AMD; retina

1. Introduction

Semenogelin proteins I and II are the major secretory products from the glandular epithelium of the seminal vesicles and the epididymis (Bjartell et l., 1996). Semenogelin I (SgI) is a non-glycosylated protein with a molecular mass of 50KDa (Lilja et al., 1989; Lilja and Lundwall, 1992). Semenogelin II (SgII) has a molecular mass of 63KDa (Lilja and Lundwall, 1992); it has a potential site for N-linked glycosylation. Approximately half of the SgII molecules in seminal plasma are glycosylated, yielding two molecular species with an apparent mass difference of 5KDa (Lilja and Laurell, 1985). Studies have indicated a role of semenogelin proteins (Sgs) related to capacitation and motility of sperm (Robert and Gagnon, 1996, de Lamirande et al., 2001; de Lamirande., 2007). More recently, high Zn^{2+}-binding capacity of

---

both SgI and SgII (Jonsson et al., 2005) was demonstrated, suggesting that Sgs might function as important regulators of extracellular Zn^{2+} homeostasis.

Recently, Sgs expression was characterized in non-genital tissues like trachea, bronchi, skeletal muscle cells, and cells in the central nervous system (Lundwall et al., 2002), suggesting additional yet unknown functions for these molecules. Our recent studies of normal human retina showed that both Sgs are found in this tissue (Bonilha et al., 2006).

Earlier clinical trial data found a significant decrease in the progression of age-related macular degeneration (AMD) in individuals supplemented with antioxidants and zinc (Age-related eye disease study research group, 2001; Clemons et al., 2005; Schmidt-Erfurth, 2005). The cellular targets in AMD are the RPE and macular photoreceptors (Penfold et al., 2001). Our observations that Sgs are localized to photoreceptors and the RPE may point to a function related to the ability of these cells to sequester Zn^{2+}- for protection against AMD. In this regard, we decided to define the distribution of Sgs in the eyes from donors with diagnosed AMD.

The purpose of this investigation was to define the distribution of SgI in the eyes from donors with diagnosed AMD and to compare this with the distribution in normal eyes. We found that the content of SgI in the AMD eyes was substantially lower than that observed in the normal retina.

2. Material and methods

2.1. Human eye tissue

Donor eyes were obtained from the Cleveland Eye Bank or through the Foundation for Fighting Blindness Eye Donor Program (Owings Mills, MD). Tissue from 20 different donors was analyzed. The donor ages varied between 35 and 97. The interval between death and tissue processing varied between 4 and 14 hours. The records received from the eye banks stated the donor eyes as AMD and non-AMD. Upon dissection the eyes were imaged and further classified as AMD or not. There were 3 eyes with GA, 2 with end-stage AMD displaying fibrovascular scar and the remaining eyes were either stage 2 or 3; no eyes had CNV. Control eyes did not have any drusen in the macular area. The immunocytochemistry and Western analysis is exempt of IRB approval.

2.2. Preparation of human RPE and retina lysates

RPE cells were isolated using the protocol initially described (Nakata et al., 2005) with mechanical removal of the retina and brushing of the RPE from the choroid. RPE cells were pelleted down, the PBS was removed and the fresh PBS containing protease inhibitors was added to the cells. The RPE cells were kept at −80°C until used. When ready to use, RPE lysates were diluted 1:1 with 2X radioimmunoprecipitation buffer (RIPA) (0.2% SDS, 2% Triton X100, 2% deoxycholate, 0.15M NaCl, 4mM EDTA, 50mM Tris pH 7.4) containing a cocktail of protease and phosphatase inhibitors (Sigma, St. Louis, MO, USA). Pieces of retinas collected from human donor eyes were collected into eppendorff tubes and lysed in 1X RIPA buffer. Cells were lyzed for 1 h at 4°C in the rotator, centrifuged for 10 min at 14000rpm and the supernatants were transferred to clean tubes and the protein concentration was determined using the MicroBCA kit (Pierce Biotechnology, Inc., Rockford, IL) according to the manufactures' directions.

2.3 Western blot analysis of lysates

40μg of protein of each sample was boiled in SDS sample buffer (62.5 mMTris-HCl (pH 6.8), 25% glycerol, 0.01% bromophenol blue, and 2% SDS), separated on a 10–20% Novex®-Tris-Glycine gel (Invitrogen Corporation, Carlsbad, CA) and electro-transferred to Immobilon

PVDF membranes (Millipore, Bedford, MA) using a Bio-Rad Semi-Dry Electrophoretic Transfer Cell (20 min transfer at 18 volts). Positive control was unliquefied seminal fluid in buffer containing 4M urea. Membranes were incubated with antibodies to SgI (cross reactivity with SgII ~ 5%) in Blotto A buffer (20 mM Tris/HCl, 0.9% NaCl, 0.05% Tween 20 (TBST), 5% skimmed milk) for 1h. Protein detection was performed with secondary antibodies conjugated to peroxidase and visualized using chemiluminescence Reagent Plus (NEN™ Life Science Products, Inc., Boston, MA) detection system. PVDF membranes were exposed to film, films were scanned and figures were composed using Adobe Photoshop 5.5.

The gels were stained with Gelcode Blue (Pierce), after partial transfer to PVDF membranes to serve as a reference for the load homogeneity of the samples as previously described (Bando et al., 2007). Briefly, both gel and blot were digitized using a densitometer, and the density of the gel and bands was measured and transferred to pixels using Quantity One 4.2.3. A rectangular area was drawn around the most intense band signal in the scanned blots and used as a template to measure the pixel intensity in each band. A rectangular area was drawn around each gel lanes and used to determine the number of pixels in these areas. Plotted signals represent pixel intensity for each band subtracted from the background signal. The total protein pixel density from each donor lane stained with Gelcode Blue in the transferred gel was quantitated. The previously determined number of pixels in the Western blot was divided by the pixels in the Gelcode Blue lane, and these then were used to establish the pixel count per sample. The average pixel count was determined as a mean of all the AMD and non-AMD samples. Standard deviation, standard error and t-test were calculated and are presented in Section 3.

2.4. Immunohistology of tissue

To determine the localization of SgI in AMD eyes, immunohistochemical assays were performed using cryo and paraffin sections of human eyes and paraffin section of isolated human Bruch's membrane/choroid in the peri-macular area. Eye pieces were cut and fixed by immersion in 4% paraformaldehyde made in PBS for 3h at 4°C. For isolated Bruch's membrane-choroid a 2X10-mm strip was isolated from the eyecups as previously described (Bando et al., 2007) and fixed by immersion in 4% formaldehyde freshly prepared from paraformaldehyde in phosphate buffer at pH 7.2 overnight. Non-AMD drusen was isolated from the perimacular area of the eyes while AMD drusen was isolated from the macular area. The isolated Bruch's membrane/choroid with drusen and retinas were then dehydrated through a series of ethanol solutions and embedded in paraffin using an automated tissue processor (Leica Microsystems TP1020, Benneck Burn, IL). 7–8μm sections were cut on a Leica RM2125 microtome (Leica Microsystems) and sections were collected on Superfrost/Plus Slides (Fisher Scientific, Pittsburg, PA). Sections were stretched on the slides on water and adhered to the slides by room temperature incubation overnight followed by 2hs incubation in a HI1210 slide warmer at 60°C (Fisher Scientific). Prior to labeling, paraffin was removed through two consecutive xylene incubations for 10 min. Next the tissues were gradually re-hydrated by sequential incubation on ethanol 100, 90, 70, 50 and 30% for 5 min. each and processed for peroxidase-DAB labeling as previously described (Bonilha et al., 2006). After rehydration to PBS, sections were subjected to heat-mediated antigen retrieval by pressure cooking in 10mM citric acid buffer, pH 6.0. Sections were probed with previously described rabbit antibodies to SgI in 5% BSA, PBS and 0.3% Triton-X100 overnight at 4°C (Bjartell et al., 1996; Malm et al., 1996). The controls omitted the antibodies. Sections were washed, incubated with secondary antibody conjugated to biotin for 1h at RT, washed, and incubated with avidin in PBS for 30 min, then developed with DAB for 2 minutes. The sections were examined with a Zeiss Axiophot light microscope and the images were digitized using a Hamamatsu CCD camera.

For cryosectioning, eye pieces of retina-RPE-choroid tissue were fixed as described above, quenched with 50mM NH_4Cl made in PBS for 1h at 4°C, infused successively with 15% and 30% sucrose made in the same buffer and with Tissue-Tek "4583" (Miles Inc., Elkhart, IN). 10–12μm cryosections were cut on a cryostat HM 505E (Microm, Walldorf, Germany) equipped with a CryoJane Tape-Transfer system (Instrumedics, Inc., Hackensack, NJ, USA). For labeling, sections were blocked in PBS supplemented with 0.3mM $CaCl_2$ + 1mM $MgCl_2$ + 1% BSA (PBS/CM/BSA) for 30 min, and incubated with the antibodies to SgI. Cell nuclei were labeled with TO-PRO®-3 iodide (Molecular Probes). Secondary antibody (goat anti-rabbit IgG; 1:1000) was labeled with Alexa Fluor 488 (green). Sections were analyzed using a Leica laser scanning confocal microscope (TCS-SP2, Leica, Exton, PA). A series of 1μm *xy* (*en face*) sections were collected. Each individual *xy* image of the retinas stained represents a three-dimensional projection of the entire cryosection (sum of all images in the stack). Microscopic panels were composed using Adobe Photoshop 5.5 (Adobe, San Jose, CA).

3. Results

3.1 Immunolocalization of SgI reduced in the retinas of AMD donors

To dissect the molecular localization of SgI in the neural retina of AMD donors, eyes were processed for cryosectioning (Fig. 1A to C) and paraffin embedding (Fig. 1D, E) followed by immunohistochemistry. The distribution of SgI was analyzed both in the retinal perimacular area of non-AMD human donors (Fig. 1A, D) and in the retinas of human donors previously diagnosed with AMD (Fig. 1B, C, E). Analysis of the AMD eye sections showed that SgI immunoreactivity is significantly reduced in all layers of the retina when compared to the non-AMD eye sections. Specifically, reduced labeling was still observed in the ganglion cells and photoreceptors inner and outer segments of the AMD eyes (Fig. 1B, C). The SgI labeling was almost completely abolished from end-stage AMD retinas with fibrovascular scar (Fig. 1C). Due to the high autofluorescence levels in the RPE/choroid layer these cells were analyzed by DAB reaction (Fig. 1D and E). A significant decrease in the SgI labeling of the RPE from AMD retinas (Fig. 1E) was observed when compared to the non-AMD control RPE (Fig. 1D).

3.2. Immunolocalization of SgI is decreased in the drusen of AMD donors

It is accepted that the pathogenesis of AMD involves changes of the RPE/Bruch's membrane and underlying choriocapillaris. To further understand the molecular localization of SgI we analyzed the immunoreactivity of SgI in the Bruch's membrane/choroid of AMD samples. Comparison of the AMD samples (Fig. 2F) showed that SgI staining is significantly reduced in the drusen from the AMD donor when compared to the non-AMD eyes (Fig. 2B). Control sections (Fig 2A and E) had the antibodies omitted. Drusen and Bruch's membrane are characterized by autofluorescence when observed in an epifluorescence microscope, in the FITC channel. This property was used to confirm drusen presence in Bruch's membrane as shown in Fig. 2 (C, D, G, H).

3.3. Sg I expression is decreased in the retina lysates of AMD donors

The differences in levels of expression of Sgs within the AMD and non-AMD retinas were addressed by Western analysis. Whole retina lysates were harvested, resolved in a SDS-PAGE and transferred to a membrane and reacted with SgI antibody (Fig. 3). Western blot using anti-SgI antibody revealed greater immunoreactivity in non-AMD (Fig. 3B, lane 1 to 4) than in AMD retinas (Fig. 3B, lane 5 to 8). After partial transfer to PVDF membranes the gels were stained with Gelcode blue to serve as a reference for the load homogeneity of the samples (Fig. 3A). Immunoblots of retina lysates obtained from AMD donor eyes demonstrated a significant decrease in SgI levels. Quantitation of these blots showed that SgI immunoreactivity was downregulated 3.7 fold lower in AMD samples when compared with non-AMD samples. These differences were statistically significant ($p < 0.0056$) (Fig. 3C).

3.4. SgI is decreased in RPE lysates from AMD donors

The differences in levels of expression of Sgs within the AMD and non-AMD RPE were addressed by Western analysis. RPE lysates were harvested, resolved in a SDS-PAGE and transferred to a membrane and reacted with SgI antibody (Fig. 4). Western blot using anti-SgI antibody revealed greater immunoreactivity in non-AMD (Fig. 4B) than in AMD retinas (Fig. 4D). Immunoblots of RPE lysates obtained from AMD donor eyes demonstrated a significant decrease in SgI levels. Quantitation of these blots showed that SgI immunoreactivity was downregulated 5.6 fold lower in AMD samples compared with non-AMD samples (Fig. 4E). These differences were statistically significant ($p < 0.0001$).

It is important to notice that both the Western blot analysis and the immunohistochemistry analysis indicated higher levels of immunoreactivity present in non-AMD than in the AMD tissues.

4. Discussion

For many years Sg was believed to be present only in the male genital tract and to originate exclusively from seminal vesicles (Robert and Gagnon, 1996). However, with time and the development of more sensitive methods, the presence of SgI and SgII transcripts was demonstrated in several tissues throughout the human body as well as in several malignant tissues and cell lines (Hienonen et al., 2005; Lundwall et al., 2002; Rodrigues et al., 2001; Zhang et al., 2003). Recently, we have shown the presence of both SgI and SgII in human retina and RPE lysates. Moreover, the Sgs distribution in the human eye tissues was associated with the choroid, RPE, photoreceptor cells, cells in the inner nuclear layer, and ganglion cell layer. In the photoreceptor cells, Sgs were observed in the inner and outer segments of both cones and rods and in the IPM (Bonilha et al., 2006). In the present study we confirmed the presence of SgI in the retina of both non-AMD and AMD eyes. However, a significant decrease in the labeling of SgI was observed throughout the retina in the ganglion cell layer, cells in the inner nuclear layer, the photoreceptors, RPE and choroid of the AMD donor eyes. It was recently reported that both SgI and II display high Zn^{2+}-binding capacity (Jonsson et al., 2005), suggesting that Sgs might function as important regulators of extracellular Zn^{2+} homeostasis. Our data suggests a possible function related to the ability of photoreceptors and RPE cells to sequester Zn^{2+} for protection against disease progression in AMD. Another possibility could be that the Sgs function as extracellular storage reservoirs of Zn^{2+}, wherefrom it could be easily and rapidly mobilized for various purposes. Low Sg levels in AMD, whether due to increased catabolism or decreased synthesis, could then perhaps be compensated for by increasing the diary intake of Zn^{2+}.

Zinc is the second most abundant trace element in the human body and the most abundant in the eye where it plays a key role in the metabolism of the retina (Karcioglu, 1982). A randomized, placebo-controlled two years clinical trial showed that zinc supplementation reduced the risk of AMD development (Newsome et al., 1988). This early report was supported by the Age-Related Eye Disease Study (AREDS) clinical trial that found that long-term (~ 6 years) intake of zinc, alone or with anti-oxidants, significantly decreased the progression of AMD and reduced the rate of moderate vision loss in individuals (Age-related eye disease study research group, 2001; Clemons et al., 2005; Schmidt-Erfurth, 2005) suggesting that zinc deficiency is a suspected risk for AMD. The cellular targets in AMD are the RPE and macular photoreceptors (Penfold et al., 2001). Photoreceptors and RPE specifically were shown to be affected in Zn^{2+} deficiency assays (Leure-duPree and McClain, 1982; Miceli et al., 1999). Moreover, studies on human eyes showed a correlation between low cytoplasmic Zn^{2+} concentrations in RPE cells and signs of AMD (Newsome et al., 1994). Our observations showed that SgI is significantly reduced but still observed in AMD photoreceptors and RPE

cells. Further studies are necessary to understand if Sgs expression is correlated to the Zn^{2+} level in AMD retinas.

The formation of lipid and protein rich sub-RPE deposits, found both in the periphery and macula, has been suggested to be a risk factor in AMD. In the present study we failed to detect SgI in drusen from AMD donors using our SgI antibody. However, SgI was recently identified in senile seminal vesicle amyloid, a common gender-specific localized form of fibril-related pathology found in older men (Linke et al., 2005). This same study has shown that SgI rendered amyloidogenic as a consequence of aging is only detected by a new SgI-reactive antibody but not by several SgI common antibodies. Amyloid β has been identified in AMD drusen (Anderson et al., 2004; Yoshida et al., 2005). A consequence of the low Sgs levels could be that Zn^{2+} binds to other extracellular proteins such as beta-amyloid, complement factor H, serum albumin and crystallins, known to bind Zn^{2+} (Lengyel et al., 07). This new interaction might lead to the accumulation of Zn^{2+} in sub-RBE deposits. Future studies will address if age-related amyloid SgI is present in AMD drusen and its role in AMD pathology.

In conclusion, we report here a significant decrease in SgI content in the retina, RPE and Bruch's membrane/choroid of AMD donors.

References

Age-Related Eye Disease Study Research Group. A randomized placebo-controlled, clinical trial of high-dose supplementation with vitamins C, E beta carotene and zinc for age-related macular degeneration, vision loss: AREDS Report N°8. Arch Ophthalmol 2001;119:1417–1436. [PubMed: 11594942]

Anderson DH, Talaga KC, Rivest AJ, Barron E, Hageman GS, Johnson LV. Characterization of β amyloid assemblies in drusen: the deposits associated with aging and age-related macular degeneration. Exp Eye Res 2004;78:243–256. [PubMed: 14729357]

Bando H, Shadrach KG, Rayborn ME, Crabb JW, Hollyfield JG. Clathrin and adaptin accumulation in drusen, Bruch's membrane and choroid in AMD and non-AMD donor eyes. Exp Eye Res 2007;84:135–142. [PubMed: 17097084]

Bjartell A, Malm J, Moller C, Gunnarsson M, Lundwell A, Lilja H. Distribution and tissue expression of semenogelin I and II in man as demonstrated by in situ hybridization and immunocytochemistry. J Androl 1996;17:17–26. [PubMed: 8833737]

Bonilha VL, Rayborn ME, Shadrach KG, Lundwall A, Malm J, Bhattacharya SK, Crabb JW. Characterization of semenogelin proteins in the human retina. Exp Eye Res 2006;83:120–127. [PubMed: 16545373]

Clemons TE, Milton RC, Klein R, Seddon JM, Ferris FL 3rd. Risk factors for the incidence of Advanced Age-Related Macular Degeneration in the Age-Related Eye Disease Study (AREDS) AREDS report no. 19. Ophthalmology 2005;112:533–539. [PubMed: 15808240]

de Lamirande E. Semenogelin, the main protein of semen coagulum, regulates sperm function. Semin Thromb Hemost 2007;33:60–68. [PubMed: 17253191]

de Lamirande E, Yoshida K, Yoshiike TM, Iwamoto T, Gagnon C. Semenogelin, the main protein of semen coagulum, inhibits human sperm capacitation by interfering with the superoxide anion generated during this process. J Androl 2001;22:672–679. [PubMed: 11451365]

Hienonen T, Sammalkorpi H, Enholm S, Alhopuro P, Barber TD, Lehtonen R, Nupponen NN, Lehtonen H, Salovaara R, Mecklin JP, Jarvinen H, Koistinen R, Arango D, Launonen V, Vogelstein B, Karhu A, Aaltonen LA. Mutations in two short noncoding mononucleotide repeats in most microsatellite-unstable colorectal cancers. Cancer Res 2005;65:4607–4613. [PubMed: 15930278]

Jonsson M, Linse S, Frohm B, Lundwall A, Malm J. Semenogelins I and II bind zinc and regulate the activity of prostate-specific antigen. Biochem J 2005;387:447–453. [PubMed: 15563730]

Karcioglu ZA. Zinc in the eye. Surv Ophthalmol 1982;27:114–122. [PubMed: 6755784]

Lengyel I, Flinn JM, Peto T, Linkous DH, Cano K, Bird AC, Lanzirotti A, Frederickson CJ, van Kuijk FJGM. High concentration of zinc in sub-retinal pigment epithelial deposits. Exp Eye Res 2007;84:772–780. [PubMed: 17313944]

Leure-duPree AE, McClain CJ. The effect of severe zinc deficiency on the morphology of the rat retinal pigment epithelium. Invest Ophthalmol Vis Sci 1982;23:425–434. [PubMed: 6288611]

Lilja H, Abrahamsson PA, Lundwall A. Semenogelin, the predominant protein in human semen. Primary structure and identification of closely related proteins in the male accessory sex glands and on the spermatozoa. J Biol Chem 1989;264:1894–1900. [PubMed: 2912989]

Lilja H, Laurell CB. The predominant protein in human seminal coagulate. Scand J Clin Lab Invest 1985;45:635–641. [PubMed: 2866578]

Lilja H, Lundwall A. Molecular cloning of epididymal and seminal vesicular transcripts encoding a semenogelin-related protein. Proc Natl Acad Sci U S A 1992;89:4559–4563. [PubMed: 1584792]

Linke RP, Joswig R, Murphy CL, Wang S, Zhou H, Gross U, Rocken C, Westermark P, Weiss DT, Solomon A. Senile seminal vesicle amyloid is derived from semenogelin I. J Lab Clin Med 2005;145:187–193. [PubMed: 15962837]

Lundwall A, Bjartell A, Olsson AY, Malm J. Semenogelin I and II, the predominant human seminal plasma proteins, are also expressed in non-genital tissues. Mol Hum Reprod 2002;8:805–810. [PubMed: 12200457]

Malm J, Hellman J, Magnusson H, Laurell CB, Lilja H. Isolation and characterization of the major gel proteins in human semen, semenogelin I and semenogelin II. Eur J Biochem 1996;238:48–53. [PubMed: 8665951]

Miceli MV, Tate DJ Jr, Alcock NW, Newsome DA. Zinc deficiency and oxidative stress in the retina of pigmented rats. Invest Ophthalmol Vis Sci 1999;40:1238–1244. [PubMed: 10235558]

Nakata K, Crabb JW, Hollyfield JG. Crystallin distribution in Bruch's membrane-choroid complex from AMD and age-matched donor eyes. Exp Eye Res 2005;80:821–826. [PubMed: 15939038]

Newsome DA, Swartz M, Leone NC, Elston RC, Miller E. Oral zinc in macular degeneration. Arch Ophthalmol 1988;106:192–198. [PubMed: 3277606]

Newsome DA, Tate DJ Jr, Alcock NW, Oliver PD. Zinc content of human retinal pigment epithelium (RPE) declines with age. Invest Ophthalmol Vis Sci 1994;35 (Suppl):1768.

Penfold PL, Madigan MC, Gillies MC, Provis JM. Immunological and aetiological aspects of macular degeneration. Prog Retin Eye Res 2001;20:385–414. [PubMed: 11286898]

Robert M, Gagnon C. Purification and characterization of the active precursor of a human sperm motility inhibitor secreted by the seminal vesicles: identity with semenogelin. Biol Reprod 1996;55:813–821. [PubMed: 8879494]

Rodrigues RG, Panizo-Santos A, Cashel JA, Krutzsch HC, Merino MJ, Roberts DD. Semenogelins are ectopically expressed in small cell lung carcinoma. Clin Cancer Res 2001;7:854–860. [PubMed: 11309333]

Schmidt-Erfurth U. Nutrition and retina. Dev Ophthalmol 2005;38:120–147. [PubMed: 15604621]

Yoshida T, Ohno-Matsui K, Ichinose S, Sato T, Iwata N, Saido TC, Hisatomi T, Mochizuki M, Morita I. The potential role of amyloid β in the pathogenesis of age-related macular degeneration. J Clin Invest 2005;115:2793–2800. [PubMed: 16167083]

Zhang Y, Wang Z, Liu H, Giles FJ, Lim SH. Pattern of gene expression and immune responses to Semenogelin 1 in chronic hematologic malignancies. J Immunother 2003;26:461–467. [PubMed: 14595213]
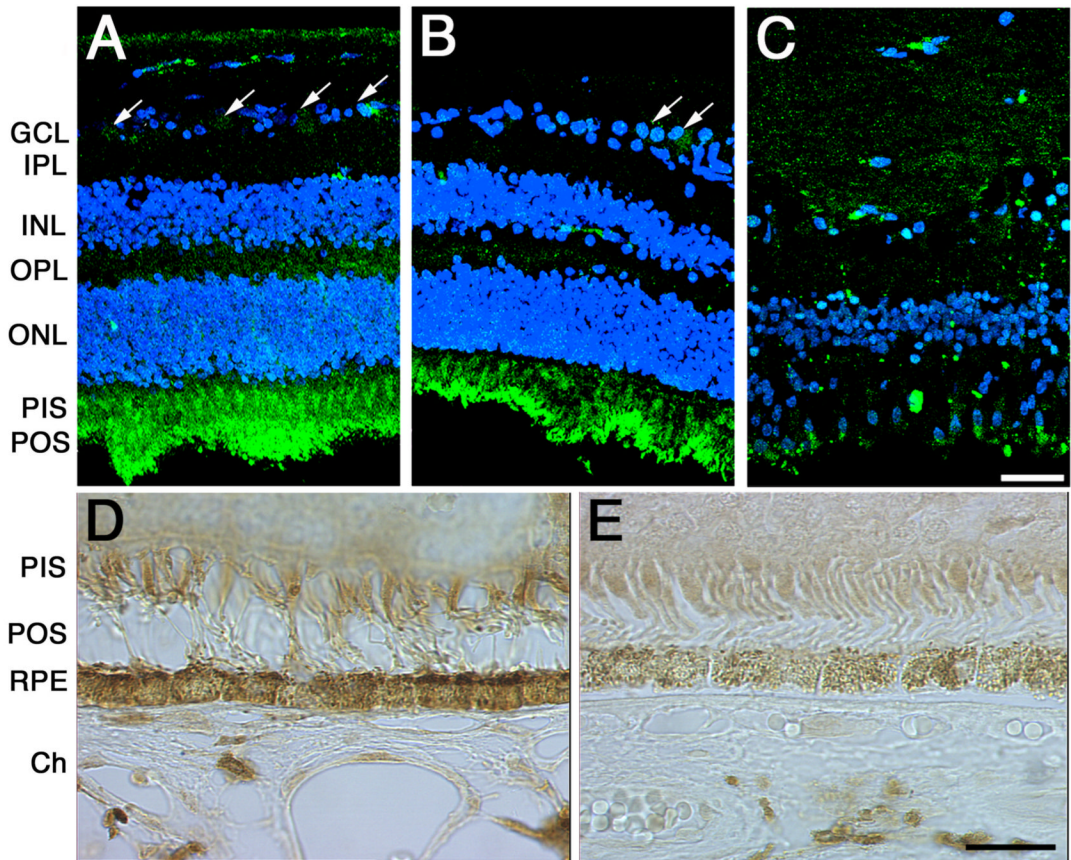
Fig. 1. SgI localization is low in the retinas of AMD donors
SgI staining is significantly reduced in all layers of the AMD retina when compared to the non-AMD eyes. Specifically, reduced labeling was observed in the photoreceptors and RPE cells. 5 control and 8 AMD donors were analyzed. Human cryosections of human donors previously diagnosed with AMD (B, C, E,) and non-AMD eyes (A, D) were probed with SgI antibody in 5% BSA, PBS and 0.3% Triton-X100 overnight at 4°C. Sections were washed, incubated with fluorophore- (A to C) or peroxidase-conjugated (D, E) secondary antibody. The controls (not shown) were omitted the antibodies and did not display any labeling. Non-AMD control retinas displayed SgI in the choroid, RPE, photoreceptor cells, cells in the inner nuclear layer, and ganglion cell layer, while in the AMD retinas SgI was mostly confined to the photoreceptor cells (B). Ch, choroid; RPE, retinal pigment epithelium, PIS, photoreceptor inner segments; POS, photoreceptor outer segments; ONL, outer nuclear layer; OPL, outer plexiform layer; INL, inner nuclear layer; IPL, inner plexiform layer; GCL, ganglion cell layer. Arrows= ganglion cells; bars (A to C)= 40μm, (D, E)=200μm.
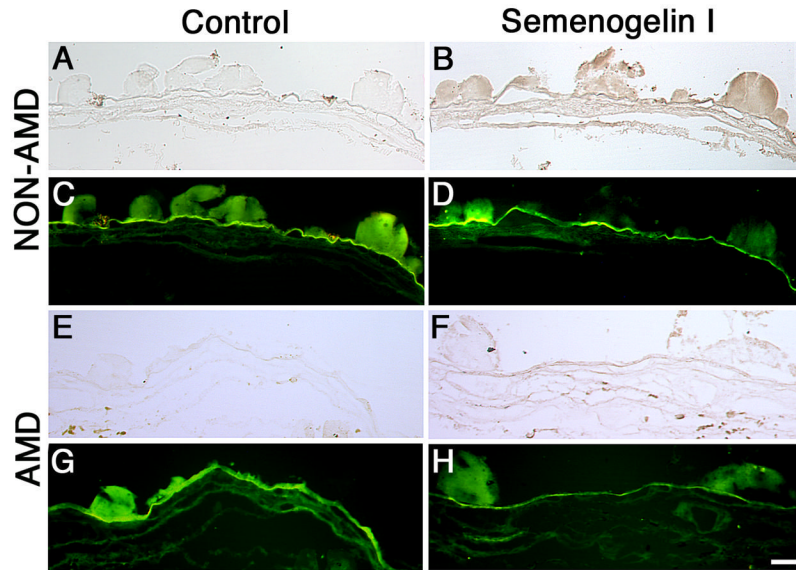
Fig. 2. SgI localization is low in the drusen of AMD donors
SgI staining is significantly reduced in the drusen from the AMD donors. 5μm paraffin sections of isolated Bruch's membrane and choroid from a human donor previously diagnosed with AMD (E–H) and non-AMD eyes (A–D) were probed with SgI antibody in 5% BSA, PBS and 0.3% Triton-X100 overnight at 4°C. Sections were washed, incubated with secondary antibody, conjugated to biotin for 1h at RT, washed, and incubated with avidin in PBS for 30 min, then developed with DAB for 2 minutes. The controls (A, C, E, G) were omitted the antibodies and did not display any labeling. The sections were examined in bright-field (A, B, E, F) or FITC channel (C, D, G, H). Observation of the samples in the FITC channel revealed the autofluorescence of the Bruch's membrane and drusen. 5 control and 8 AMD donors were analyzed. Bar = 200μm.

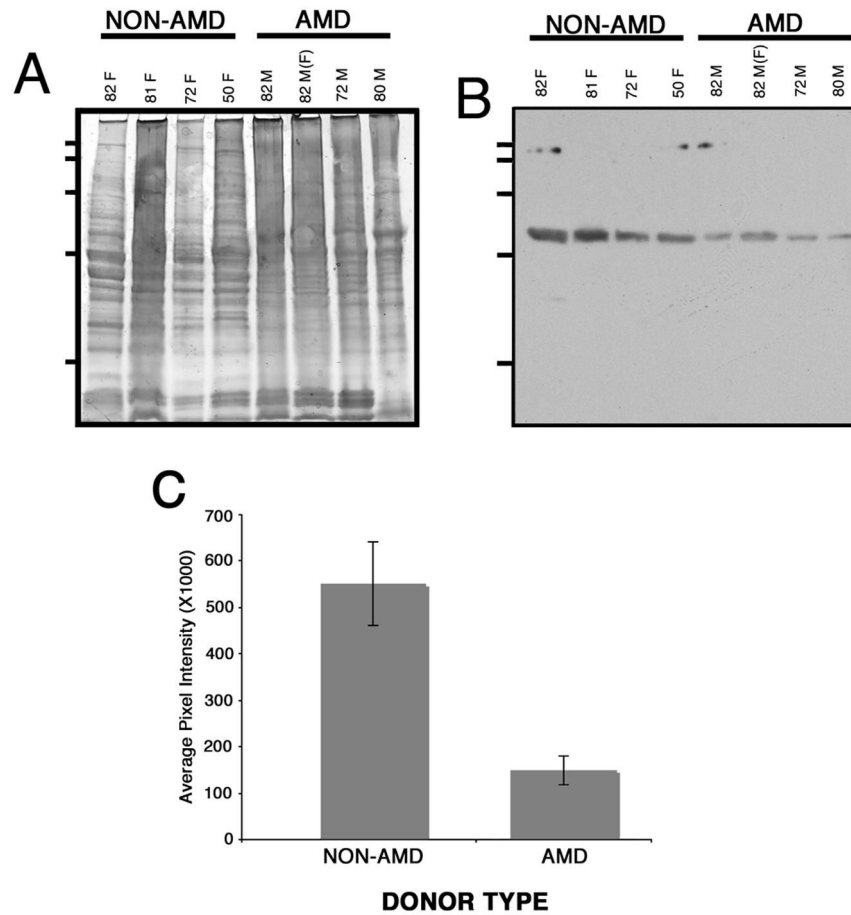**Fig. 3. SgI expression is low in the retinas of AMD donors**
Retinas from several human donors (9 control and 9 AMD donors) previously diagnosed with AMD and non-AMD samples were harvested, lysed in RIPA buffer (150mM NaCl, 25mM Tris, pH 7.4, 2mM EDTA, 1% Triton X-100, 1% deoxycholate, 0.1% SDS) supplemented with 1mM PMSF, protease and phosphatase cocktail inhibitors (SIGMA). 40μg of protein of each sample was separated on a 10–20% SDS gel, transferred to PVDF membranes and probed with antibodies specific to SgI followed by ECF detection of immunoreactivity (B). The gels were stained with Gelcode blue after partial transfer to PVDF membranes to serve as a reference for the load homogeneity of the samples (A). The age and gender of the donors are indicated on top of each lane; all donors were caucasians. Membranes were exposed to film, and films were scanned. In C, a rectangular area was drawn around the most intense band signal and used as a template to measure the signal intensity in each band using the volume analysis report macro from Quantity One 4.2.3. Plotted signals represent mean pixel intensity for AMD and non-AMD samples ± error bars. SgI immunoreactivity was approximate 3.7 fold lower in AMD samples compared with non-AMD samples (p < 0.0056 by Student's t-test). (F) in sample 82M denotes the fovea of that donor.
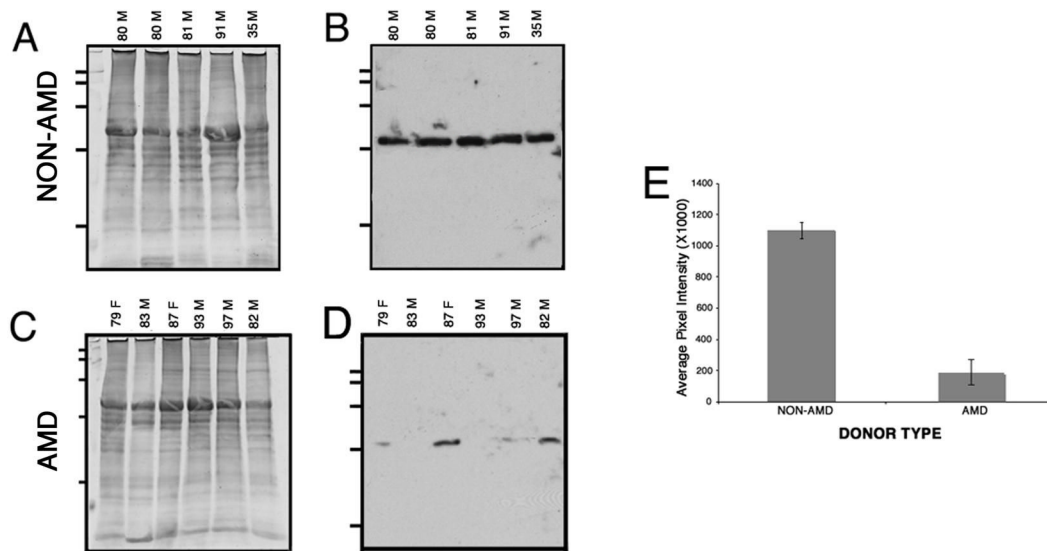
Fig. 4. SgI is significantly lower in RPE lysates from AMD donors
RPE lysates from several human donors (9 control and 9 AMD donors) previously diagnosed with AMD and non-AMD samples were harvested, lysed in RIPA buffer (150mM NaCl, 25mM Tris, pH 7.4, 2mM EDTA, 1% Triton X-100, 1% deoxycholate, 0.1% SDS) supplemented with 1mM PMSF, protease and phosphatase cocktail inhibitors (SIGMA). 40μg of protein of each sample was separated on a 10–20% SDS gel, transferred to PVDF membranes and probed with antibodies specific to SgI followed by ECF detection of immunoreactivity (B and D). The gels were stained with Gelcode blue after partial transfer to PVDF membranes to serve as a reference for the load homogeneity of the samples (A and C). The age and gender of the donors are indicated on top of each lane; all donors were caucasians. Membranes were exposed to film, and films were scanned. In E, a rectangular area was drawn around the most intense band signal and used as a template to measure the signal intensity in each band using the volume analysis report macro from Quantity One 4.2.3. Plotted signals represent mean pixel intensity for AMD and non-AMD samples ± error bars. SgI immunoreactivity was approximate 5.6 fold lower in AMD samples compared with non-AMD samples ($p < 0.0001$ by Student's t-test).